

## PRIORITY COMMUNICATION

## Selective Oxidation of Dimethylether to Formaldehyde on Small Molybdenum Oxide Domains

Haichao Liu and Enrique Iglesia<sup>1</sup>*Department of Chemical Engineering, University of California at Berkeley, Berkeley, California 94720*

Received January 7, 2002; revised January 28, 2002; accepted February 11, 2002

MoO<sub>x</sub> species dispersed as small domains on Al<sub>2</sub>O<sub>3</sub>, ZrO<sub>2</sub>, and SnO<sub>2</sub> catalyze the oxidative conversion of dimethylether to formaldehyde with high primary selectivity (80–98% HCHO, CH<sub>3</sub>OH-free basis) at low temperatures (500–550 K). The reaction appears to proceed via redox cycles using lattice oxygen and turnover rates increase with the size and reducibility of MoO<sub>x</sub> domains. Dimethylether conversion rates (per g) and formaldehyde selectivities at 513 K are significantly higher than those reported previously on various catalysts at significantly higher temperatures (620–880 K). © 2002 Elsevier Science (USA)

**Key Words:** dimethylether oxidation; formaldehyde synthesis; molybdenum oxide.

## 1. INTRODUCTION

Formaldehyde is used as an intermediate in the synthesis of many chemicals (1). It is currently produced via oxidative dehydrogenation of methanol on iron molybdates and Ag-based catalysts (2, 3). Reaction pathways and catalyst requirements for methanol conversion to formaldehyde have been previously addressed (3, 4). Methanol reactions involve rate-limiting C–H bond cleavage of surface methoxide intermediates (CH<sub>3</sub>O). These methoxide species can also form via cleavage of the weak C–O–C linkages in dimethylether (CH<sub>3</sub>OCH<sub>3</sub>; DME) on metal oxides (5, 6), but only a few patents have reported effective catalysts for oxidative conversion of DME to formaldehyde (7–10). To some extent, this reflects the higher historical cost of DME relative to methanol, but recent studies have shown that DME can be produced economically from synthesis gas (11, 12). DME is not toxic or corrosive and it can be transported as a chemical intermediate or as a potential fuel within existing and emerging LPG infrastructures (11, 12).

These considerations led us to examine the catalytic chemistry involved in the conversion of DME to formalde-

hyde on active metal oxides. Initial exploratory studies identified MoO<sub>x</sub> and VO<sub>x</sub> as preferred catalytic species and well-dispersed active oxide domains, present predominantly as two-dimensional structures, as the best compromise between the reactivity and the accessibility of the active sites at oxide surfaces. We focus here on MoO<sub>x</sub> domains supported at near monolayer surface densities on Al<sub>2</sub>O<sub>3</sub>, ZrO<sub>2</sub>, or SnO<sub>2</sub>. These materials show formaldehyde formation rates significantly higher than previously reported (7–10), even at much lower temperatures than in previous studies.

## 2. EXPERIMENTAL

Supported MoO<sub>x</sub> catalysts were prepared by incipient wetness impregnation of ZrO(OH)<sub>2</sub>, SnO<sub>2</sub>, Al<sub>2</sub>O<sub>3</sub>, or MgO with aqueous (NH<sub>4</sub>)<sub>2</sub>Mo<sub>2</sub>O<sub>8</sub> (99%, Aldrich) solutions (13–15). ZrO(OH)<sub>2</sub> was prepared by hydrolysis of aqueous zirconyl chloride solutions (>98%, Aldrich) using NH<sub>4</sub>OH (14.8 N), followed by drying in ambient air at 393 K overnight. SnO<sub>2</sub> was prepared by hydrolysis of tin (IV) chloride pentahydrate (98%, Alfa Aesar) with NH<sub>4</sub>OH (14.8 N) and then treated in dry air at 773 K for 3 h. The γ-Al<sub>2</sub>O<sub>3</sub> (Degussa, AG) support was used without further treatment. MgO was prepared by contacting MgO (>98%, Aldrich) with deionized water at 355–365 K for 4 h and then treating it in dry air at 773 K for 8 h. All samples were dried at 373 K in ambient air after impregnation and then treated in dry air at 773 K for 3 h. Bulk MoO<sub>3</sub> was prepared by decomposition of (NH<sub>4</sub>)<sub>2</sub>Mo<sub>2</sub>O<sub>8</sub> (99%, Aldrich) in dry air at 773 K for 3 h.

Dimethylether reactions were carried out in a fixed-bed quartz microreactor using catalyst samples (0.3 g) diluted with quartz powder (1 g) in order to prevent local high temperatures caused by the exothermic reaction. The reactant mixture consisted of 80 kPa DME, 18 kPa O<sub>2</sub>, and 2 kPa N<sub>2</sub>; N<sub>2</sub> was used as an internal standard. Reactants and products were analyzed by on-line gas chromatography (Hewlett–Packard 6890 GC) using flame ionization and

<sup>1</sup> To whom correspondence should be addressed. Fax: (510) 642-4778. E-mail: [iglesia@cchem.berkeley.edu](mailto:iglesia@cchem.berkeley.edu).

thermal conductivity detectors and methyl-silicone capillary and Porapak Q packed columns. Rates and selectivities were measured as a function of DME conversion, which was changed by varying the reactant residence time. DME conversion rates and formaldehyde selectivities were extrapolated to zero reactant residence time in order to obtain primary rates and selectivities. DME conversion rates and selectivities are reported in two forms in the results shown in Table 1. One approach considers CH<sub>3</sub>OH as a DME conversion product. The other approach reports rates and selectivities on a CH<sub>3</sub>OH-free basis. This latter description seems appropriate in view of the reversible nature of DME conversion to methanol and of the pathways available for the ultimate conversion of both CH<sub>3</sub>OH and DME to HCHO.

### 3. RESULTS AND DISCUSSION

Table 1 shows catalytic results obtained at 513 K on MoO<sub>x</sub> domains supported on Al<sub>2</sub>O<sub>3</sub>, ZrO<sub>2</sub>, and SnO<sub>2</sub> at similar Mo surface densities (6.4–7.0 Mo atoms/nm<sup>2</sup>). Primary reaction rates (normalized by catalyst mass) were much higher on these three catalysts than on previously reported catalysts (7–10), even at the lower temperatures used here. Rates were higher on SnO<sub>2</sub> and ZrO<sub>2</sub> supports than on Al<sub>2</sub>O<sub>3</sub>, but primary formaldehyde selectivities (CH<sub>3</sub>OH-free) were nearly 100% on MoO<sub>x</sub>/Al<sub>2</sub>O<sub>3</sub>. MoO<sub>x</sub> domains supported on MgO did not give measurable DME

conversion rates, apparently because of the formation of mixed metal oxide structures, which are unable to undergo the reduction–oxidation cycles required for DME catalytic turnovers at these reaction temperatures. Pure supports also showed very low DME conversion rates. A MoO<sub>3</sub> sample with relatively low surface area gave low DME conversion rates (per gram). Its areal rate was similar to those on MoO<sub>x</sub>/Al<sub>2</sub>O<sub>3</sub> and 2–6 times lower than on MoO<sub>x</sub> supported on ZrO<sub>2</sub> or SnO<sub>2</sub>. Formaldehyde was not detected on MoO<sub>3</sub> at 513 K, because of the low DME conversions attained. At higher temperatures (593 K), the primary HCHO selectivity was 52.9% (on a CH<sub>3</sub>OH-free basis) on bulk MoO<sub>3</sub>. MoO<sub>x</sub>/Al<sub>2</sub>O<sub>3</sub> was the most selective catalyst for DME conversion to HCHO. Its primary HCHO selectivity was 79.1% (98.1%, CH<sub>3</sub>OH-free basis) and CO and CO<sub>2</sub> (CO<sub>x</sub>) were not detected at all as primary products.

A parallel study showed that the catalytic properties of these MoO<sub>x</sub> domains depend sensitively on their size and local structure, which were varied by changing the Mo surface density on Al<sub>2</sub>O<sub>3</sub> (1.6–11.3 Mo/nm<sup>2</sup>) and ZrO<sub>2</sub> (2.2–30.6 Mo/nm<sup>2</sup>) supports. Primary DME reaction rates increased from 2.3 to 5.7 mol/g atom Mo-h as Mo surface densities increased from 1.6 to 7.0 Mo/nm<sup>2</sup> on Al<sub>2</sub>O<sub>3</sub> (Table 2). These rates increased from 0.6 to 12.2 mol/g atom Mo-h as surface densities increased from 2.2 to 6.4 Mo/nm<sup>2</sup> on ZrO<sub>2</sub>. On both ZrO<sub>2</sub> and Al<sub>2</sub>O<sub>3</sub>, DME reactions reached maximum rates (per Mo) at intermediate Mo surface densities (6–7 Mo/nm<sup>2</sup>).

TABLE 1

DME Oxidation Rates and Selectivities on Supported MoO<sub>x</sub> Catalysts at 513 K (80.0 kPa DME, 18 kPa O<sub>2</sub> and 2 kPa N<sub>2</sub>), on Bulk MoO<sub>3</sub>, and on Previously Reported Catalysts

Catalyst (MoO <sub>3</sub> wt%)	Surface area (m <sup>2</sup> /g)	Mo surface density (Mo/nm <sup>2</sup> )	Temperature (K)	DME conversion rate <sup>a</sup> (mmol/ g <sub>cat</sub> -h)	DME conversion rate <sup>a</sup> (mol/g atom Mo-h)	DME conversion rate <sup>a</sup> (10 <sup>-5</sup> mol/ m <sup>2</sup> -h)	Selectivity (%) <sup>a</sup>					Reference
							CH <sub>3</sub> OH	HCHO	MF <sup>b</sup>	DMM <sup>c</sup>	CO <sub>x</sub> <sup>d</sup>	
MoO <sub>3</sub> /ZrO <sub>2</sub> (20.7%)	136.3	6.4	513	17.6 (13.6) <sup>a</sup>	12.2 (9.4)	12.9	22.6	53.4 (69.0)	16.8 (21.7)	0.3 (0.4)	6.9 (8.9)	This study
MoO <sub>3</sub> /SnO <sub>2</sub> (7.2%)	46.5	6.5	513	18.4 (16.0)	36.5 (31.7)	39.6	13.1	67.3 (77.6)	9.6 (11.1)	0 (0)	9.8 (11.3)	This study
MoO <sub>3</sub> /Al <sub>2</sub> O <sub>3</sub> (15.0%)	90.0	7.0	513	5.8 (4.7)	5.7 (4.6)	6.6	19.7	79.9 (98.1)	1.6 (1.9)	0 (0)	0 (0)	This study
MoO <sub>3</sub> /MgO (24.0%)	171.2	5.8	513	Not detected	Not detected	—	—	—	—	—	—	This study
MoO <sub>3</sub>	3.3	—	513	0.2	—	6.1	6.0	0	0	0	94.0	This study
Ag <sup>e</sup>	—	—	887	10.5	—	—	—	45.8	0	0	30.7	10
Bi–Mo–FeO <sub>x</sub> <sup>f</sup>	—	—	773	3.1	—	—	0	46.0	0	0	54.0	7
Bi–Mo–CuO <sub>x</sub> <sup>f</sup>	—	—	773	2.9	—	—	0	43.0	0	0	55.0	8
Mn nodules <sup>f</sup>	~230	—	623	1.7	—	0.7	—	49.0	—	—	—	9

<sup>a</sup> The data in parentheses are reported on a CH<sub>3</sub>OH-free basis by excluding CH<sub>3</sub>OH as a reaction product in view of its reactivity in formaldehyde synthesis and its tendency to dehydrate to reform CH<sub>3</sub>OCH<sub>3</sub>.

<sup>b</sup> MF: methyl formate.

<sup>c</sup> DMM: dimethoxymethane.

<sup>d</sup> CO<sub>x</sub>: CO + CO<sub>2</sub>.

<sup>e</sup> Reactants: 59.9 kPa DME, 8.5 kPa O<sub>2</sub>, 31.6 kPa N<sub>2</sub>.

<sup>f</sup> Reactants: 5.0 kPa DME, 20.0 kPa O<sub>2</sub>, 75.0 kPa N<sub>2</sub>.

The structure of supported MoO<sub>x</sub> catalysts has been previously examined using various methods (13, 14, 16–19). Saturation polymolybdate surface densities are ~5 Mo/nm<sup>2</sup>, and the relative concentrations of isolated monomolybdates, two-dimensional polymolybdates, and bulk MoO<sub>3</sub> depend on the Mo surface density, the identity of the support, and the temperature of the thermal treatments. At the intermediate Mo surface densities in the samples used in this study, ZrO<sub>2</sub> and Al<sub>2</sub>O<sub>3</sub> supports are predominately covered with two-dimensional polymolybdate structures (13, 14). X-ray diffraction and Raman, UV–visible, and X-ray absorption spectroscopies did not detect MoO<sub>3</sub> crystallites for surface densities below 7 Mo/nm<sup>2</sup> on these samples (13, 14). In this Mo surface density range, most, if not all, MoO<sub>x</sub> species are accessible at surfaces and DME conversion rates per Mo atom are equivalent to rates per exposed MoO<sub>x</sub> structure (i.e., turnover rates). Therefore, the higher reaction rates attained with increasing surface density reflect a higher reactivity of exposed MoO<sub>x</sub> as the size and dimensionality of MoO<sub>x</sub> domains increase with increasing Mo surface density. The larger domains formed at higher MoO<sub>x</sub> surface densities (inferred from their absorption edge energy in the UV–visible spectra (13, 14)) appear to undergo the redox cycles required for DME conversion to HCHO more rapidly than isolated monomolybdate species or smaller two-dimensional polymolybdate domains.

This interpretation is consistent with the observed increase in the rate of incipient reduction of Mo<sup>6+</sup> to Mo<sup>4+</sup> as MoO<sub>x</sub> surface density increases in these samples. The peak temperature in these reduction profiles decreased by ~70 K as the Mo surface density increased from 0.4 to 6.5 Mo/nm<sup>2</sup> on ZrO<sub>2</sub>. Ultimately, DME conversion rates (per Mo) decreased at even higher Mo surface densities (>10 Mo/nm<sup>2</sup>), because the formation of three-dimensional MoO<sub>3</sub> clusters leads to increasingly inaccessible MoO<sub>x</sub> species.

Primary formaldehyde selectivities increased monotonically with increasing Mo surface density; they reached values of 88.3 and 98.1% (CH<sub>3</sub>OH-free) on MoO<sub>x</sub>/ZrO<sub>2</sub> and MoO<sub>x</sub>/Al<sub>2</sub>O<sub>3</sub>, respectively, at 30.6 and 11.3 Mo/nm<sup>2</sup>. On MoO<sub>x</sub>/ZrO<sub>2</sub>, both methylformate and CO<sub>x</sub> selectivities decreased with increasing Mo surface density (to ~5% for each product), while CH<sub>3</sub>OH selectivities remained nearly constant with changes in Mo surface density. On MoO<sub>x</sub>/Al<sub>2</sub>O<sub>3</sub>, methanol selectivities decreased as the Al<sub>2</sub>O<sub>3</sub> support became covered with MoO<sub>x</sub> species, and the primary formaldehyde selectivity concurrently increased with increasing Mo surface density (Table 2). Methylformate and CO<sub>x</sub> primary selectivities were very low on all Al<sub>2</sub>O<sub>3</sub>-supported MoO<sub>x</sub> samples. The CH<sub>3</sub>OH-free primary HCHO selectivity was 95–98% on Mo/Al<sub>2</sub>O<sub>3</sub> samples with 1.6 to 11.3 Mo/nm<sup>2</sup> (Table 2). High HCHO selectivities were also obtained on VO<sub>x</sub>/Al<sub>2</sub>O<sub>3</sub> catalysts at these reaction conditions. The CH<sub>3</sub>OH-free primary HCHO selectivity on VO<sub>x</sub>/Al<sub>2</sub>O<sub>3</sub> (8.0 V/nm<sup>2</sup>) was 99.6% and the primary DME reaction rate was 6.8 mol/g atom V-h (20).

TABLE 2

Effects of Surface Density of MoO<sub>x</sub>/Al<sub>2</sub>O<sub>3</sub> Catalysts on Primary DME Reaction Rates and Primary Products at 513 K (80.0 kPa DME, 18 kPa O<sub>2</sub>, and 2 kPa N<sub>2</sub>)

Mo surface density (Mo/nm <sup>2</sup> )	Rate <sup>a</sup> (mol/g atom Mo-h)	Selectivity (%) <sup>a</sup>				
		CH <sub>3</sub> OH	HCHO	MF <sup>b</sup>	DMM <sup>c</sup>	CO <sub>x</sub> <sup>d</sup>
1.6	2.3 (1.5) <sup>a</sup>	34.1	62.8 (95.2)	2.5 (3.7)	0 (0)	0.8 (1.2)
3.4	3.9 (2.8)	27.0	70.5 (96.5)	2.4 (3.2)	0 (0)	0.2 (0.3)
4.5	5.2 (4.1)	22.1	76.3 (97.9)	1.5 (1.9)	0 (0)	0.1 (0.1)
7.0	5.7 (4.6)	19.5	79.1 (98.1)	1.6 (1.9)	0 (0)	0 (0)
11.3	3.8 (3.1)	19.4	79.0 (98.0)	1.6 (1.9)	0.1 (0.1)	0 (0)

<sup>a</sup> The data in parentheses are reported on a CH<sub>3</sub>OH-free basis by excluding CH<sub>3</sub>OH as a reaction product in view of its reactivity in formaldehyde synthesis and its tendency to dehydrate to reform CH<sub>3</sub>OCH<sub>3</sub>.

<sup>b</sup> MF: methyl formate.

<sup>c</sup> DMM: dimethoxymethane.

<sup>d</sup> CO<sub>x</sub>: CO + CO<sub>2</sub>.

The high HCHO selectivities observed on MoO<sub>x</sub>/Al<sub>2</sub>O<sub>3</sub> (7.0 Mo/nm<sup>2</sup>) at low DME conversions decreased slightly and DME conversion rates remained nearly constant as DME conversions increased with decreasing reactant space velocity (Fig. 1). For example, the HCHO selectivity

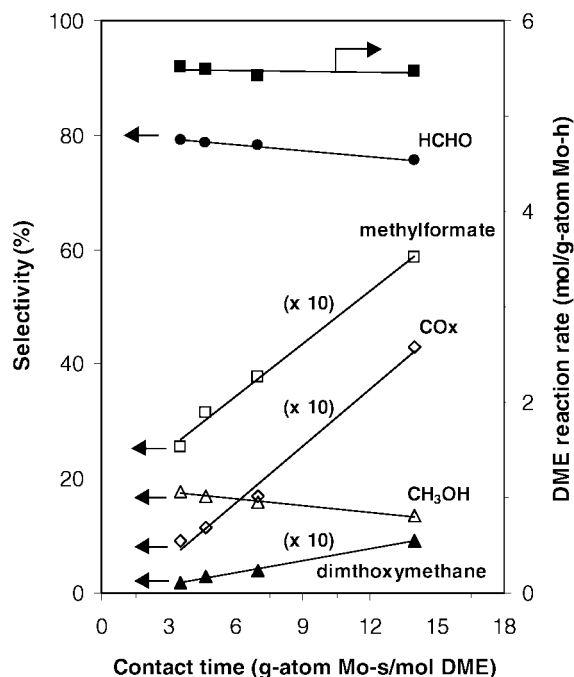


FIG. 1. Rates and selectivities for dimethylether oxidation on MoO<sub>x</sub>/Al<sub>2</sub>O<sub>3</sub> (7.0 Mo/nm<sup>2</sup>) at 513 K as a function of reactant residence time (80 kPa CH<sub>3</sub>OCH<sub>3</sub>, 18 kPa O<sub>2</sub>, 2 kPa N<sub>2</sub>).

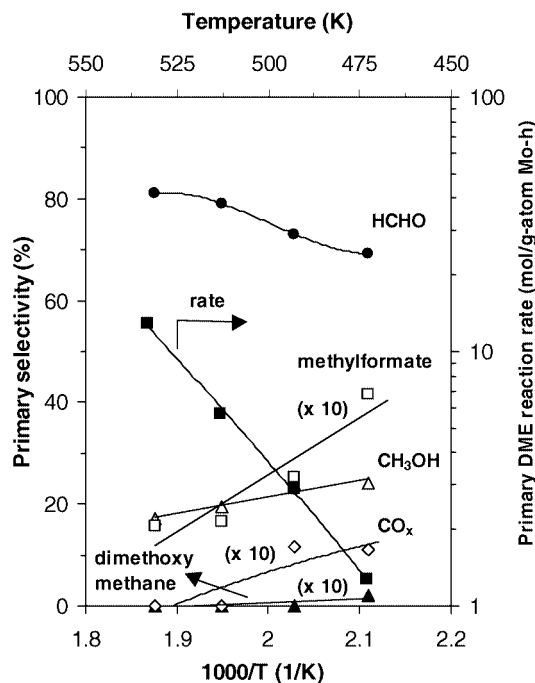


FIG. 2. Rates and selectivities for dimethylether oxidation on MoO<sub>x</sub>/Al<sub>2</sub>O<sub>3</sub> (7.0 Mo/nm<sup>2</sup>) as a function of reaction temperature (80 kPa CH<sub>3</sub>OCH<sub>3</sub>, 18 kPa O<sub>2</sub>, 2 kPa N<sub>2</sub>).

(CH<sub>3</sub>OH-free) decreased from 94.4% to 87.2% as DME conversions increased from 0.9% to 3.5% (CH<sub>3</sub>OH-free). These data suggest that secondary reactions of HCHO to form methylformate or CO<sub>x</sub> are significantly slower than primary oxidation of DME to form HCHO on MoO<sub>x</sub>/Al<sub>2</sub>O<sub>3</sub>. This is likely to reflect the stronger nature of the C–H bonds in HCHO compared with the C–O–C bonds initially cleaved during DME conversion to HCHO.

We have also explored the effects of temperature on DME reaction rates and on formaldehyde selectivity (Fig. 2; 473–533 K). Homogeneous DME reactions were not detected in this temperature range, but some reaction products were detected at temperatures above 593 K even in the absence of a catalyst. DME reaction rates and primary formaldehyde selectivities on MoO<sub>x</sub>/Al<sub>2</sub>O<sub>3</sub> increased with increasing reaction temperature (Fig. 2). DME reaction rates increased from 1.3 to 12.9 mol/g-atom Mo-h as the temperature increased from 473 K to 533 K, while primary HCHO selectivities concurrently increased from 91.2 to 98.1% (CH<sub>3</sub>OH-free). Even at the highest temperature, primary CO<sub>x</sub> and dimethoxymethane (DMM) selectivities were very low, and primary methylformate selectivities were ~2.0% (CH<sub>3</sub>OH-free). When CH<sub>3</sub>OH was included as a reaction product in the selectivity calculations, the selectivity to HCHO increased with increasing temperature, because of a preferential increase in HCHO formation rates relative to CH<sub>3</sub>OH formation rates.

The catalytic properties of supported MoO<sub>x</sub> domains are compared with those for several patented catalysts in Table 1. Ag-based catalysts similar to those used in methanol oxidation to formaldehyde showed DME conversion rates of 10.5 mmol/g-h (at 17.2% DME conversion) at 887 K with low formaldehyde selectivities (45.8%) and significant selectivities to CO<sub>x</sub> (31.7%) and light alkanes (19.5%) (10). This reaction rate (at 887 K) resembled those reported here for MoO<sub>x</sub>/ZrO<sub>2</sub> and MoO<sub>x</sub>/SnO<sub>2</sub> at 513 K; it is only slightly higher than those measured on MoO<sub>x</sub>/Al<sub>2</sub>O<sub>3</sub> at these lower temperatures. These supported MoO<sub>x</sub> catalysts exhibit higher HCHO selectivities and lower CO<sub>x</sub> selectivities than Ag catalysts at similar DME conversions. On a MoO<sub>x</sub>/ZrO<sub>2</sub> (8.4 Mo/nm<sup>2</sup>) sample treated in air at 873 K, HCHO and CO<sub>x</sub> selectivities were 57.7 and 14.7%, respectively, at 13.7% DME conversion; the reaction rate was 29.5 mmol/g-h at 513 K (CH<sub>3</sub>OH-free basis). Bi–Mo–Fe and Bi–Mo–Cu mixed oxides and Mn nodules also catalyze DME oxidation to formaldehyde, but they are considerably less active than the MoO<sub>x</sub>-based catalysts reported here (Table 1) (7–9).

The high dispersion and reducible nature of the MoO<sub>x</sub> domains in our samples lead to a high density of very reactive redox sites and to much higher DME conversion rates than previously reported. Detailed mechanistic studies and structural characterization of these materials suggest that the reaction proceeds via redox cycles using lattice oxygen atoms. These pathways appear to involve methoxide intermediates and C–H bond activation and hydrogen transfer reactions leading to HCHO and CH<sub>3</sub>OH from these intermediates. The strong effects of the support and of the oxide domain size on the structure and electronic properties of dispersed MoO<sub>x</sub> domains are being examined using spectroscopic, site titration, and transient techniques.

#### ACKNOWLEDGMENTS

This study was supported by BP as part of the Methane Conversion Cooperative Research Program at the University of California at Berkeley. The authors thank Dr. Kaidong Chen for the synthesis of some of the supported MoO<sub>x</sub> samples. The authors also acknowledge helpful technical discussions with Drs. Theo Fleisch and John Collins of BP.

#### REFERENCES

- Walker, J. K., "Formaldehyde." Reinhold, New York, 1964.
- Lefferts, L., van Ommen, J. G., and Ross, J. R. H., *Appl. Catal.* **23**, 385 (1986).
- Tatibouet, J. M., *Appl. Catal. A Gen.* **148**, 213 (1997).
- Deo, G., and Wachs, I. E., *J. Catal.* **146**, 323 (1994).
- Hara, M., Kawamura, M., Kondo, J. N., Domen, K., and Maruya, K., *J. Phys. Chem.* **100**, 14,462 (1996).
- Ouyang, F., and Yao, S., *J. Phys. Chem.* **104**, 11,253 (2000).
- Lewis, R. M., Ryan, R. C., and Slaugh, L. H., U.S. Patent 4,442,307, 1984.
- Lewis, R. M., Ryan, R. C., and Slaugh, L. H., U.S. Patent 4,439,624, 1984.

9. Lewis, R. M., Ryan, R. C., and Slaugh, L. H., U.S. Patent 4,435,602, 1984.
10. Hagen, G. P., and Spangler, M. J., U.S. Patent 6,265,528, 2001.
11. Fleisch, T. H., Basu, A., Gradassi, M. J., and Masin, J. G., *Stud. Surf. Sci. Catal.* **107**, 117 (1997).
12. Shikada, T., Ohno, Y., Ogawa, T., Ono, M., Mizuguchi, M., Tomura, K., and Fujimoto, K., *Stud. Surf. Sci. Catal.* **119**, 515 (1998).
13. Chen, K., Xie, S., Iglesia, E., and Bell, A. T., *J. Catal.* **189**, 421 (2000).
14. Chen, K., Xie, S., Bell, A. T., and Iglesia, E., *J. Catal.* **198**, 232 (2001).
15. Liu, H., and Iglesia, E., to be published.
16. Mestl, G., and Srinivasan, T. K. K., *Catal. Rev. Sci. Eng.* **40**, 451 (1998).
17. Wachs, I. E., *Catal. Today* **27**, 437 (1996).
18. Kiszfaludi, G., Leyrer, J., Knozinger, H., and Prins, P., *J. Catal.* **130**, 192 (1991).
19. Xie, Y. C., and Tang, Y. Q., *Adv. Catal.* **37**, 1 (1990).
20. Liu, H., and Iglesia, E., to be published.